Mena invasive (Mena^{INV}) promotes multicellular streaming motility and transendothelial migration in a mouse model of breast cancer

Evanthia T. Roussos[1,*], Michele Balsamo[2], Shannon K. Alford[2], Jeffrey B. Wyckoff[1,3], Bojana Gligorijevic[1], Yarong Wang[1], Maria Pozzuto[4], Robert Stobezki[5], Sumanta Goswami[1,5], Jeffrey E. Segall[1], Douglas A. Lauffenburger[2], Anne R. Bresnick[4], Frank B. Gertler[2,*] and John S. Condeelis[1,3,*]

[1]Department of Anatomy and Structural Biology, Albert Einstein College of Medicine, Bronx, NY 10461, USA
[2]David H. Koch Institute for Integrative Cancer Research, Massachusetts Institute of Technology, Cambridge, MA 02139, USA
[3]Gruss Lipper Biophotonics Center, Albert Einstein College of Medicine, Bronx, NY 10461, USA
[4]Department of Biochemistry, Albert Einstein College of Medicine, Bronx, NY 10461, USA
[5]Department of Biology, Yeshiva University, New York, NY 10033, USA
*Authors for correspondence (evanthia.roussos@med.einstein.yu.edu; fgertler@mit.edu; john.condeelis@einstein.yu.edu)

Accepted 18 February 2011
Journal of Cell Science 124, 2120-2131

doi:10.1242/jcs.086231

Summary

We have shown previously that distinct Mena isoforms are expressed in invasive and migratory tumor cells in vivo and that the invasion isoform (Mena^{INV}) potentiates carcinoma cell metastasis in murine models of breast cancer. However, the specific step of metastatic progression affected by this isoform and the effects on metastasis of the Mena11a isoform, expressed in primary tumor cells, are largely unknown. Here, we provide evidence that elevated Mena^{INV} increases coordinated streaming motility, and enhances transendothelial migration and intravasation of tumor cells. We demonstrate that promotion of these early stages of metastasis by Mena^{INV} is dependent on a macrophage–tumor cell paracrine loop. Our studies also show that increased Mena11a expression correlates with decreased expression of colony-stimulating factor 1 and a dramatically decreased ability to participate in paracrine-mediated invasion and intravasation. Our results illustrate the importance of paracrine-mediated cell streaming and intravasation on tumor cell dissemination, and demonstrate that the relative abundance of Mena^{INV} and Mena11a helps to regulate these key stages of metastatic progression in breast cancer cells.

Key words: Breast cancer, Cell motility, Intravital imaging, Metastasis, Transendothelial migration

Introduction

Cell motility is essential for many aspects of metastasis; however, few molecular markers exist that can predict the migratory potential of a tumor cell in vivo. Intravital multiphoton imaging in animal models can be used to characterize carcinoma and stromal cell behavior within intact primary tumors in detail (Condeelis and Segall, 2003; Wang et al., 2007; Egeblad et al., 2008; Kedrin et al., 2008; Andresen et al., 2009; Perentes et al., 2009). Such imaging approaches yield direct information at single-cell resolution and permit quantification of cell motility, interactions between tumor and stromal cells, and direct observation of invasion, intravasation and extravasation. In mammary tumors, this technology was used to describe the microenvironments in which tumor cells invade, migrate and intravasate, and revealed essential roles for macrophages in these events (reviewed in Condeelis and Segall, 2003; Condeelis and Pollard, 2006; Yamaguchi et al., 2006; Kedrin et al., 2007). In particular, chemotaxis of tumor cells toward macrophages is essential for invasion in mouse primary mammary tumors (Wyckoff et al., 2004; Goswami et al., 2005), whereas chemotaxis of tumor cells toward peri-vascular macrophages is essential for intravasation (Wyckoff et al., 2007).

Expression profiling of invasive tumor cells captured from the primary tumor was used to obtain molecular information regarding the pathways mediating carcinoma cell invasion and intravasation (Wyckoff et al., 2000a; Wang et al., 2004; Wang et al., 2007). The 'invasion signature' obtained from this profile revealed sets of coordinated expression changes associated with increased invasive potential (Goswami et al., 2004; Wang et al., 2004; Wang et al., 2006; Wang et al., 2007; Goswami et al., 2009). Mena, a regulator of actin polymerization and cell migration, is upregulated in invasive tumor cells obtained from rat, mouse and human tumors (Di Modugno et al., 2006; Goswami et al., 2009; Robinson et al., 2009). Conservation of Mena upregulation in invasive tumor cells across species suggests that it plays a crucial role in metastatic progression.

In patients, Mena expression correlates with metastatic risk: relatively high Mena expression has been observed in patient samples from high-risk primary and metastatic breast tumors (Di Modugno et al., 2006), as well as cervical, colorectal and pancreatic cancers compared with low-risk cases (Gurzu et al., 2008; Pino et al., 2008; Gurzu et al., 2009). Mena is also a component of a marker for metastatic risk called TMEM (tumor micro-environment for metastasis) (Robinson et al., 2009). TMEMs are identified by co-localization of Mena-positive tumor cells, macrophages and endothelial cells, and the TMEM score predicts risk independently of clinical subtype of cancer (Robinson et al., 2009). Therefore, the contribution of Mena to metastasis is independent of clinical subtype.

These findings emphasize the importance of determining the mechanism by which Mena and its isoforms differentially affect

Journal of Cell Science

metastatic progression. Mena is a member of the Ena/VASP family of proteins and binds actin to regulate the geometry and assembly of filament networks through: (1) an anti-capping protein activity (Bear et al., 2002; Barzik et al., 2005; Hansen and Mullins, 2010) that involves binding to profilin and both G- and F-actin; (2) Mena tetramerization, and (3) reduction in the density of actin-related proteins 2 and 3 (Arp2/3)-mediated branching (Gertler et al., 1996; Barzik et al., 2005; Ferron et al., 2007; Pasic et al., 2008; Bear and Gertler, 2009; Hansen and Mullins, 2010). Alternative splicing for the Mena gene has been reported: a 19 amino acid residue insertion just after the EVH1 domain generates the Mena invasion isoform (Mena^{INV}, formerly Mena^{+++}) (Gertler et al., 1996; Philippar et al., 2008), whereas a 21 residue insertion in the EVH2 domain generates the Mena11a isoform (Di Modugno et al., 2007). A comparison of the invasive and migratory tumor cells collected in vivo, with primary tumor cells isolated from mouse, rat and human cell-line-derived mammary tumors, revealed that Mena^{INV} expression is upregulated and Mena11a is downregulated selectively in the invasive and migrating carcinoma cell population (Goswami et al., 2009). The differential regulation of Mena isoforms across species suggests that these two isoforms have important roles in invasion and metastasis.

In previous studies, we showed that expression of Mena^{INV} in a xenograft mouse mammary tumor promotes increased formation of spontaneous lung metastases from orthotopic tumors and alters the sensitivity of tumor cells to epidermal growth factor (EGF) (Philippar et al., 2008). We undertook the current study to identify the step(s) in the metastatic cascade that are affected by Mena^{INV} expression and investigate the effect of expression of the second regulated isoform, Mena11a, on metastatic progression. In particular, we dissected each step of metastatic progression to determine which steps are affected by expression of Mena^{INV} that ultimately leads to enhancement of metastatic dissemination, and whether these same steps are also affected by Mena11a expression in tumor cells.

We chose MTLn3 cells for our studies because they are well characterized with respect to tumor cell invasion, migration and metastasis (Levea et al., 2000; Sahai, 2005; Le Devedec et al., 2009; Le Devedec et al., 2010), tumor–stromal cell interactions (Sahai, 2005), TGFβ signaling in metastatic progression (Giampieri et al., 2009), and the role of Mena in breast cancer metastasis (Philippar et al., 2008; Goswami et al., 2009). MTLn3 cells are derived from the clonal selection of metastatic lung lesions from rats with mammary tumors (Neri et al., 1982). These rat mammary tumors have been characterized as estrogen-independent and they metastasize to the lymph nodes and lungs (Neri et al., 1982). Evaluation of vimentin and cytokeratins in MTLn3 mammary tumors, associated lymph nodes and lung metastases revealed that MTLn3 tumor cells are comparable to a basal-like subtype of breast cancer (Lichtner et al., 1989).

Results

Mena^{INV} promotes coordinated cell migration in vivo in the form of streams of single cells

Previously, we found that expression of Mena and Mena^{INV} increases in vivo cell motility, which we hypothesized contributes to the increased lung metastasis observed with these cells (Philippar et al., 2008). Different types of motility are thought to play diverse roles during tumor cell invasion (Wolf et al., 2003; Gaggioli et al., 2007; Ilina and Friedl, 2009; Friedl and Wolf, 2010), therefore we hypothesized that Mena^{INV} expression promotes a type of motility that supports enhanced tumor cell invasion. To address this hypothesis, we used multiphoton-based intravital imaging (IVI) to examine the types of motility displayed by tumor cells expressing the different Mena isoforms. In all tumors, we generally observed two patterns of movement: coordinated cell movement whereby the cells align and move in an ordered single file line (streaming) (Fig. 1A, top panel; supplementary material Movie 1), and random cellular movement whereby carcinoma cells move independently of other carcinoma cells in an uncoordinated manner (Fig. 1A, bottom panel; supplementary material Movie 2). Both Mena^{INV}-expressing and Mena11a-expressing tumor cells exhibited streaming and random movement in vivo. However, streaming movement was significantly more common in Mena^{INV}-expressing tumor cells in vivo (Fig. 1B). Quantification of cells moving within the primary tumor showed that Mena^{INV} expression significantly increased both random and streaming tumor cell movement compared with that seen with GFP-expressing control cells and Mena11a-expressing primary mammary tumors. Both movement types were only slightly increased in Mena11a-expressing tumor cells (Fig. 1B). To characterize streaming motility further, time-lapse images were analyzed for cell crawling (supplementary material Fig. S1A), and we used photoconversion from green to red to measure the stability of the streams over a 24-hour period (Kedrin et al., 2008). Carcinoma cell streams were observed over 24 hours after photoconversion, suggesting that streaming is a long-lived behavior (Fig. 1C) involving crawling cells (supplementary material Fig. S1A). Results from co-injection of MTLn3 cells expressing GFP–Mena11a–GFP or Cerulean–Mena^{INV} showed that the tissue architecture specific to each Mena isoform type is preserved as compared with injection of either Mena11a- or Mena^{INV}-expressing cells alone (data not shown).

Streaming cell movement is more productive than random cell movement

We studied the underlying motility parameters contributing to streaming and random movement by determining cell speed, net path length, directionality and turning frequency in vivo. In vivo, streaming cells moved significantly faster than randomly moving cells, regardless of Mena isoform expression (supplementary material Fig. S1B), with average speeds of greater than 1.9 μm/minute. All cell types participating in random movement exhibited a narrow distribution of velocities (supplementary material Fig. S1Ci), whereas cells that participated in streaming movement had a broad distribution of velocities (supplementary material Fig. S1Cii). This suggests that random cell movement is autonomous, whereas streaming cells exhibit velocities dependent on multiple cell–cell signaling interactions.

The directionality, net path length and turning frequency of a cell are measures of cell locomotion efficiency. In general, the net path length (supplementary material Fig. S1D) and directionality (supplementary material Fig. S1E) of streaming carcinoma cells in vivo were increased, whereas turning frequency was decreased (supplementary material Fig. S1F) compared with randomly moving cells. These results indicate that streaming cell movement is more efficient because cells that stream move faster, farther and turn less frequently. The increased streaming observed in vivo for cells expressing Mena^{INV} (supplementary material Fig. S1B) means that Mena^{INV}-expressing cells move more efficiently in vivo. In steady-state conditions in vitro, cells only move randomly and the Mena isoform-expressing cells did not differ significantly from each other in speed and directionality. This suggests that additional factors are required for streaming that are not present in vitro

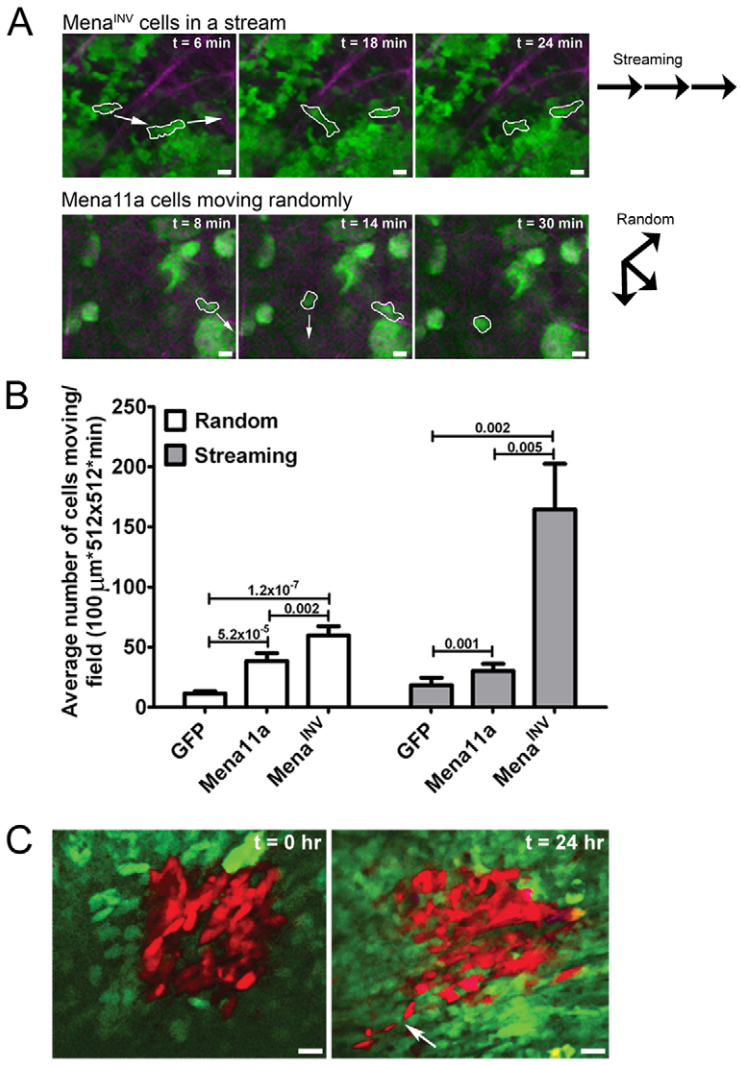

Fig. 1. Mena^{INV} promotes coordinated carcinoma cell streaming within the primary tumor significantly more than other Mena isoforms. (**A**) Multiphoton microscopy images (20×) of Mena^{INV}- and Mena11a-expressing mammary tumors in mice. Upper panels illustrate MTLn3–Cerulean–EGFP–Mena^{INV} cells at different intervals in time, moving in a stream; cells outlined in white follow the same path (direction indicated with white arrows in far left panel) as they move through the tumor. Lower panels illustrate MTLn3–Cerulean–EGFP–Mena11a cells at different intervals of time, moving randomly; cells outlined in white are moving in different directions from each other (directions indicated with white arrows in far left and middle panels). Scale bars: 25 µm. Green, Cerulean MTLn3 cells expressing either EGFP–Mena^{INV} or EGFP–Mena11a. Purple, collagen I second harmonic. Vector diagrams to the right illustrate movement patterns of streaming (top vector diagram) versus randomly moving (bottom vector diagram) cells in the panels to the left. Vector diagrams are representative of all cell types participating in either streaming or random movement. (**B**) Average number of tumors cells moving randomly (white bars) or streaming (gray bars) per field quantified from IVI of primary mammary tumors derived from mammary gland injection of cell types indicated; 30–50 fields analyzed per condition. *P* values are indicated above bars. Error bars indicate s.e.m. (**C**) Multiphoton microscopy of Mena^{INV}-expressing MTLn3 tumor cells coexpressing Dendra2 moving coordinately in a cell stream. Images taken at 20× at time 0 (image taken immediately following Dendra2 photoconversion) and 24 hours following Dendra2 photoconversion from green to red. Red area results from the same red photoconverted tumor cells in both images. White arrow, Denra2 photoconverted carcinoma cells in a stream. Green, Dendra2 in MTLn3–Mena^{INV} cells. Scale bars: 50 µm.

(supplementary material Fig. S2A,B). We investigated these additional in vivo factors and outline the results below.

In vivo invasion is enhanced by the expression of Mena^{INV} and suppressed by the expression of Mena11a

To determine whether the enhanced streaming exhibited by Mena^{INV}-expressing carcinoma cells correlates with chemotaxis-dependent invasion, we used the in vivo invasion assay to evaluate the ability of carcinoma cells to invade towards EGF in vivo (Wyckoff et al., 2000a). We showed previously that MTLn3 cells exhibit a characteristic biphasic response to EGF whereby maximal chemotactic invasion is achieved in response to 25 nM EGF (Segall et al., 1996; Wyckoff et al., 2000a). Expression of Mena^{INV} shifts this biphasic response, and maximal invasion is achieved in response to 1 nM EGF (Fig. 2A) (Philippar et al., 2008). This result demonstrates that sensitivity to EGF chemotaxis is increased in vivo and is consistent with the increased sensitivity of Mena^{INV}-expressing cells to EGF in vitro (supplementary material Fig. S3A,B) (Philippar et al., 2008). In vitro, Mena^{INV}-expressing cells exhibit protrusive activity in response to EGF concentrations as low as 0.1 nM, whereas cells expressing GFP and Mena11a did not respond to stimulation with either 0.1 or 0.5 nM EGF (supplementary material Fig. S3A,B). Importantly, Mena^{INV} expression not only sensitizes tumor cells to EGF, but also significantly increases the number of invasive cells collected with the peak concentration of EGF, which indicates more efficient cell migration (Fig. 2A). Mena11a-expressing tumors did not invade significantly above background levels in response to a broad range of EGF concentration (Fig. 2A). Thus, Mena11a and Mena^{INV} have opposite effects on chemotaxis-dependent invasion in vivo.

Expression of Mena isoforms alters paracrine loop signaling with macrophages during in vivo invasion

Using the in vivo invasion assay, tumor cells have been observed to chemotax into needles containing either EGF or colony-stimulating factor 1 (CSF1) (Wyckoff et al., 2004; Patsialou et al., 2009). This can only occur if a paracrine signaling relay is established with macrophages because, in the absence of macrophages, the chemotatic signal cannot be transmitted over long distances and few cells are collected (Wyckoff et al., 2004). Therefore, we looked at whether the tumor cell–macrophage paracrine loop is involved in the enhanced in vivo invasion of Mena^{INV}-expressing cells and the suppression of invasion in Mena11a-expressing cells. Both macrophages and tumor cells enter

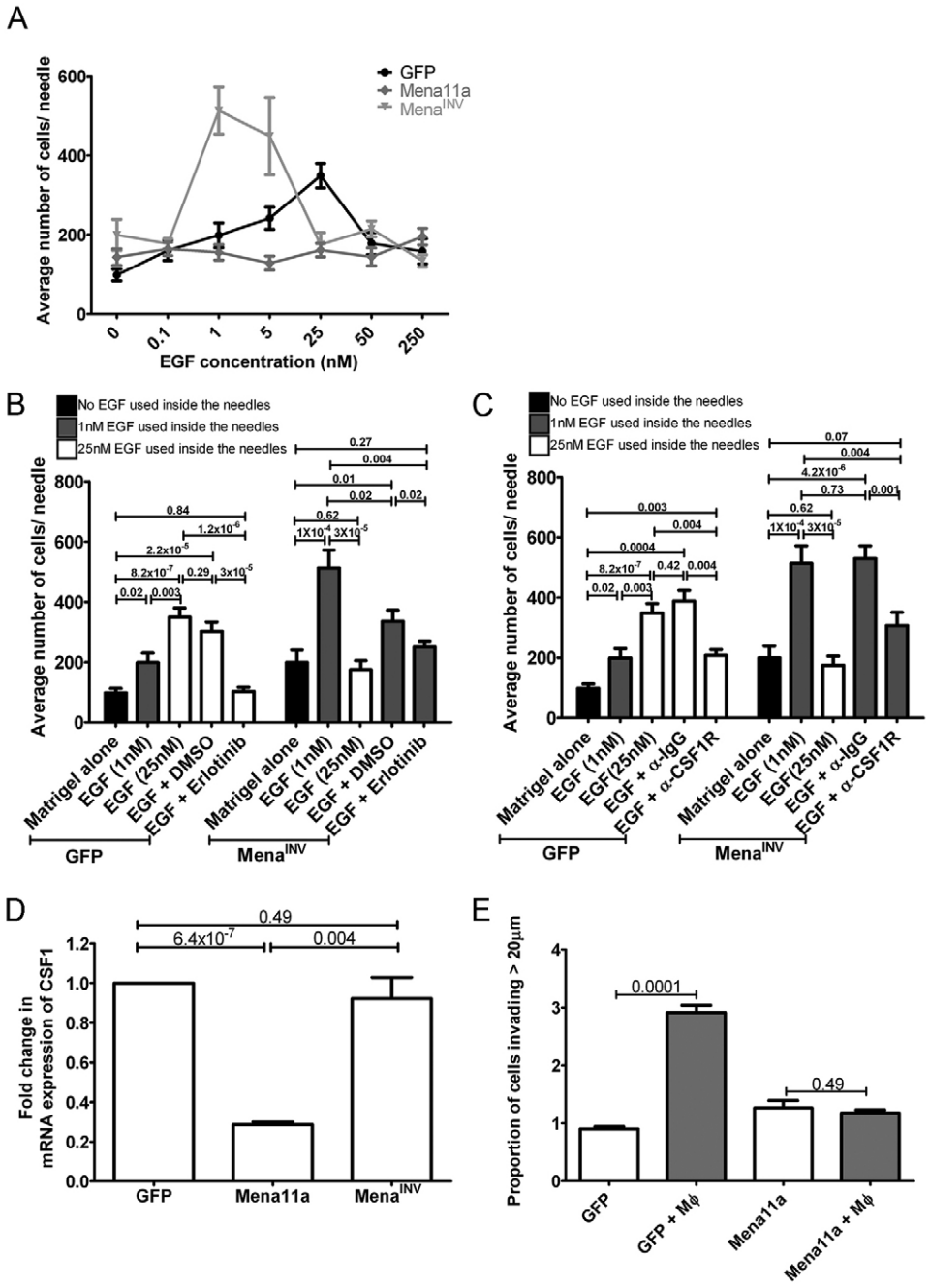

Fig. 2. Mena^{INV} and Mena11a have opposite effects on invasion in vivo and in vitro. (**A**) In vivo invasion assay: EGF dose-response curve of cells collected from primary mammary tumors derived from mammary gland injection of indicated cell types. Values represent averages of 15–25 needles per xenograft model. (**B**) In vivo invasion in the presence of Erlotinib. Cells were collected from mammary tumors derived from mammary gland injection of each cell type. Bars represent contents of 15–25 needles per xenograft model. (**C**) In vivo invasion in the presence of CSF1R-blocking antibody (α-CSF1R): Cells collected from mammary tumors derived from mammary gland injection of each cell type. Bars represent contents of 15–25 needles per xenograft model. (**D**) Real time PCR of cell lines for expression of CSF1. Each bar represents n=3 for three independent experiments. (**E**) In vitro 3D invasion assay. Proportion of GFP- and Mena11a-expressing cells invading collagen in the absence (white bars) or presence (gray bars) of macrophages. Each bar represents n=3. P values are indicated above bars. Error bars indicate s.e.m.

collection needles during in vivo invasion (Wyckoff et al., 2004), and typing of cells collected following in vivo invasion confirmed the presence of both tumor cells and macrophages in collections from tumors expressing GFP, Mena^{INV} and Mena11a (data not shown).

To assess the extent of paracrine signaling between macrophages and Mena^{INV}-expressing carcinoma cells during in vivo invasion, we performed the in vivo invasion assay in the presence of either 6.25 nM Erlotinib (Tarceva), an EGF receptor (EGFR) tyrosine kinase inhibitor, or a mouse CSF1 receptor-blocking antibody (α-CSF1R) (Wyckoff et al., 2004). In vivo invasion of both Mena^{INV}- and GFP-expressing cells was reduced to background levels in assays with Erlotinib as compared with invasion toward needles containing EGF+DMSO or EGF alone (Fig. 2B), demonstrating the requirement for EGFR-mediated stimulation for invasion. Similarly, invasion of both Mena^{INV}- and GFP-expressing cells decreased significantly with needles containing α-CSF1R as compared with invasion toward needles containing EGF+DMSO or EGF+IgG antibodies (control IgG) (Fig. 2C), thus suggesting the necessity of EGF production and signal propagation by macrophages. These results are consistent with the requirement for co-migrating macrophages in tumor cell migration, as shown in Fig. 3D and discussed below. Together, these results demonstrate the requirement for paracrine signaling between Mena^{INV}-expressing tumor cells and macrophages in vivo.

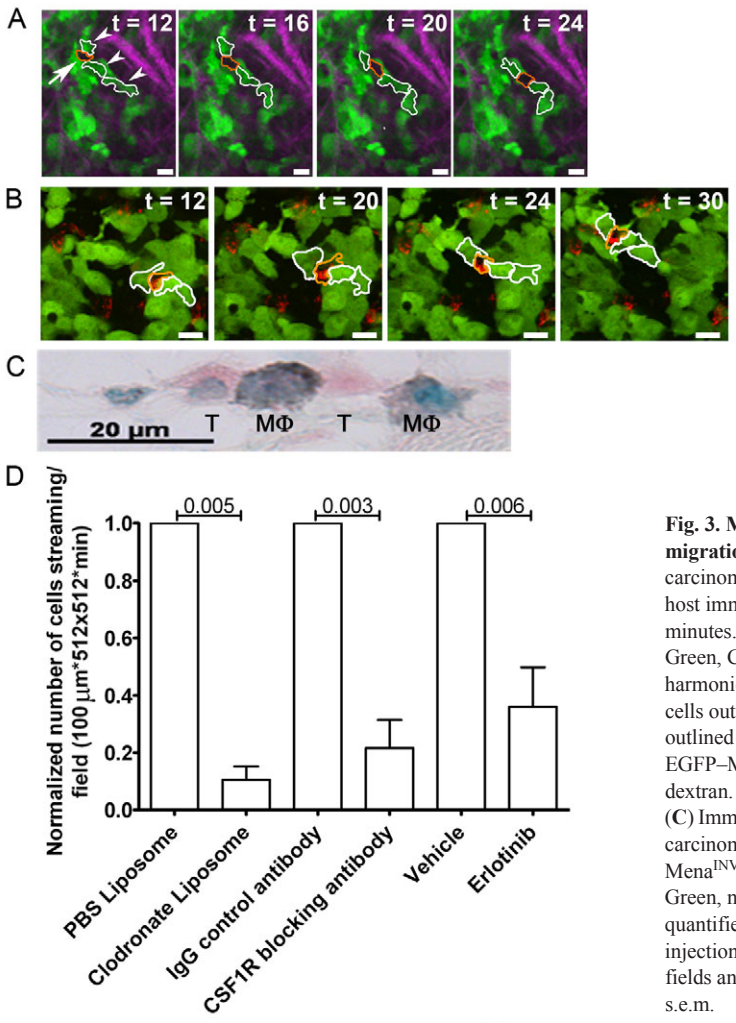

Fig. 3. Macrophages co-migrate with carcinoma cells during coordinated cell migration as part of the migratory stream. (**A**) Multiphoton microscopy of carcinoma cells (green cells outlined in white) moving coordinately in a stream with host immune cells (black shadow outlined in orange). Images taken at 20× over 30 minutes. Arrows point to host immune cells. Arrowheads point to carcinoma cells. Green, Cerulean MTLn3 cells expressing EGFP–Mena^{INV}. Purple, collagen I second harmonic. Scale bars: 25 μm. (**B**) Multiphoton microscopy of carcinoma cells (green cells outlined in white) and Texas Red dextran-labeled macrophages (red cells outlined in orange) moving in a stream. Green, Cerulean MTLn3 cells expressing EGFP–Mena^{INV}. Purple, collagen I second harmonic. Red, Texas Red-labeled dextran. Images taken at 20× over 30 minutes. Scale bars: 25 μm. (**C**) Immunohistochemistry of EGFP–Mena^{INV} primary tumor section stained for carcinoma cells (pink) and macrophages (gray), imaged at 63×. Pink, EGFP–Mena^{INV} within MTLn3–EGFP–Mena^{INV} cells. Gray, F4/80 within macrophages. Green, nuclear counterstain. (**D**) Normalized number of cells streaming per field quantified from IVI of primary mammary tumors derived from mammary gland injection of MTLn3–EGFP–Mena^{INV} treated with the indicated reagents; 30–50 fields analyzed per condition. *P* values indicated above bars. Error bars indicate s.e.m.

Both CSF1 secretion and EGF binding to the EGFR by carcinoma cells are essential components of the carcinoma cell–macrophage paracrine loop (Wyckoff et al., 2004; Patsialou et al., 2009). We used real time PCR to examine the relative mRNA expression of CSF1 and EGFR in the Mena isoform-expressing cells lines in culture to determine whether changes in the expression of these signaling molecules could contribute to the observed differences in EGF-dependent in vivo invasion (Wyckoff et al., 2004). Mena11a-expressing cells showed a fourfold decrease in CSF1 expression as compared with GFP-expressing cells, whereas CSF1 expression in Mena- and Mena^{INV}-expressing cells was unchanged (Fig. 2D). We previously reported no difference in EGFR expression in cells expressing either Mena or Mena^{INV} as compared with MTLn3 cells (Philippar et al., 2008). Cells expressing Mena11a also showed no statistical difference in expression of EGFR compared with GFP- and Mena^{INV}-expressing cells (supplementary material Fig. S4), indicating that altered receptor levels do not contribute to the altered EGF-dependent phenotypes observed in the different cell types. Thus, the inability of Mena11a-expressing cells to participate in macrophage-dependent invasion might arise in part due decreased CSF1 expression along with a reduction in direct response EGF (Fig. 2D).

To determine whether suppression of chemotaxis-dependent invasion of Mena11a-expressing tumor cells resulted from differences in the ability of these tumor cells to co-migrate with macrophages, we used a 3D invasion assay that measures macrophage-dependent co-migration of carcinoma cells with macrophages in collagen (Goswami et al., 2005). Although addition of macrophages to GFP-expressing tumor cells significantly increased 3D invasion, addition of macrophages to Mena11a-expressing cells did not significantly increase invasion (Fig. 2E). This is consistent with the reduced response to EGF and the reduced CSF1 expression levels in Mena11a-expressing cells that fall below the threshold needed to stimulate the pro-invasive macrophage behavior (Fig. 2D).

Mena^{INV}-expressing carcinoma cell streaming requires the presence of macrophages and paracrine signaling

Because the enhanced invasion of Mena^{INV}-expressing carcinoma cells depends on paracrine loop signaling with macrophages, and the paracrine loop has been shown to be required for tumor cell migration in mammary tumors (Wyckoff et al., 2004), we hypothesized that the paracrine loop also drives carcinoma cell streaming in vivo. Using IVI, we observed that multiple carcinoma cells moved in streams among host cell shadows previously

identified as immune cells and macrophages (Wyckoff et al., 2000b; Wyckoff et al., 2007) (Fig. 3A; supplementary material Movie 3). Intravenous injection of Texas Red dextran during IVI indeed confirmed the identity of the host cell shadows in tumor cell streams as macrophages, because macrophages uniquely take up dextran delivered intravenously into mammary tumors over the time interval of these experiments (Wyckoff et al., 2007) (Fig. 3B; supplementary material Movie 4). Additionally, immunohistochemistry of fixed primary tumors identified macrophages intercalated between carcinoma cells in cell streams (Fig. 3C).

To determine whether streaming required macrophages, mice were treated with clodronate liposomes 48 hours prior to IVI to decrease levels of functional macrophages (Hernandez et al., 2009). A 70% decrease in the number of Texas Red dextran-labeled macrophages was observed in animals treated with clodronate liposomes compared with those treated with PBS liposomes (supplementary material Fig. S5). IVI of primary tumors demonstrated that there were 90% fewer streaming cells in mice treated with clodronate liposomes as compared with controls, confirming the involvement of the macrophage–tumor cell paracrine loop in streaming (Fig. 3D). To confirm the involvement of the paracrine loop in streaming, mice were treated with Erlotinib 2 hours prior to IVI to block the EGFR on tumor cells (Zerbe et al., 2008) or with a CSF1R antibody 4 hours prior to IVI to block the CSF1R on macrophages (Wyckoff et al., 2007). IVI of primary tumors demonstrated that there were 65% fewer streaming cells in mice treated with Erlotinib and 80% fewer streaming cells in mice treated with α-CSF1R as compared with tumors (Fig. 3D).

Expression of Mena^{INV} in tumor cells leads to increased transendothelial migration and intravasation

Given that our data shows increased streaming (Fig. 1B) and invasion (Fig. 2A) in Mena^{INV}-expressing cells we hypothesized that expression of Mena^{INV} might also enhance intravasation to increase metastasis. Following intravenous injection of Texas Red dextran, IVI of Mena^{INV}-expressing tumors showed that tumor cell streaming was indeed directed toward blood vessels (Fig. 4A; supplementary material Movie 5). We then quantified the intravasation efficiency of tumors expressing Mena^{INV} and Mena11a using IVI of photoconverted carcinoma cells adjacent to blood vessels to determine the percentage of tumor cells intravasating over a 24-hour period (Fig. 4B) (Kedrin et al., 2008). Quantification of the change in the photoconverted tumor area 24 hours after photoconversion showed that 95% of Mena11a-expressing cells remained in the converted area as compared with 75% of carcinoma cells expressing Mena^{INV} (Fig. 4Bi,ii). Additionally, we evaluated the tumor cell blood burden to measure intravasation in vivo (Wyckoff et al., 2000b). Mice with Mena^{INV}-expressing tumors had a fourfold increase in the number of carcinoma cells in circulation compared with mice with GFP- or Mena11a-expressing tumors (Fig. 4C). Mena11a-expressing xenograft mice had similar numbers of circulating carcinoma cells as compared with GFP-expressing xenograft mice (Fig. 4C).

Given that previous studies showed that interaction between tumor cells and perivascular macrophages is required for intravasation (Wyckoff et al., 2007), and that our studies show that enhanced Mena^{INV} cell streaming and invasion are paracrine-dependent, we hypothesized that enhanced intravasation in Mena^{INV}-expressing cells might also be paracrine-dependent. To examine the minimum requirements for macrophage-assisted intravasation we used a subluminal-to-luminal transendothelial migration (TEM) assay in which we could vary the presence of macrophages to determine their need for carcinoma cell intravasation (Fig. 4D). Interestingly, less than 0.5% of carcinoma cells traversed the endothelium in the absence of macrophages, regardless of Mena isoform expression (Fig. 4E). Addition of macrophages did not enhance TEM for cells expressing GFP or Mena11a (Fig. 4E). Remarkably, in the presence of macrophages, 54% of Mena^{INV}-expressing cells traversed the endothelium, a 200-fold increase in TEM as compared with all other cell types (Fig. 4E).

To test the paracrine dependence of intravasation in vivo, we assessed the number of circulating tumor cells following functional impairment of macrophages achieved by treatment of mice with clodronate liposomes or CSF1R-blocking antibody, or impairment of tumor cells by treatment with Erlotinib. Tumors formed from injection of Mena^{INV}-expressing cells showed a significant decrease in circulating tumor cells following treatment with clodronate liposomes, CSF1R blocking antibody and Erlotinib as compared with those treated with respective controls (Fig. 4F).

Expression of Mena^{INV}, but not Mena11a, increases intravasation, dissemination and lung metastasis

To determine the mechanistic consequence of enhanced transendothelial migration and intravasation by Mena^{INV} expression or the suppression of invasion by Mena11a expression, we investigated the ability of these cells to extravasate, disseminate and metastasize to the lung. An experimental metastasis assay was used as a measure of extravasation (Xue et al., 2006). Micrometastases in the lungs were counted after intravenous injection of GFP-, Mena11a- or Mena^{INV}-expressing cells. The metastatic burden was similar for all cell lines (Fig. 5A).

Previous studies have shown that MTLn3 tumor cells forced to express Mena^{INV} show a significant increase in the number of metastases formed (Philippar et al., 2008). Thus, we asked whether dissemination of single tumor cells to the lung, a step preceding growth of macrometastases, was affected in xenograft mice derived from injection of cells expressing Mena^{INV} or Mena11a. Mice with Mena^{INV} xenografts had significantly increased carcinoma cell dissemination to the lungs compared with animals bearing either Mena11a- or GFP-expressing tumors (Fig. 5B). Mice with Mena11a xenografts had half as many cells in the lungs as mice bearing GFP-expressing tumors (Fig. 5B).

Given that Mena^{INV} expression increases tumor cell dissemination and that Mena11a expression decreases tumor cell dissemination, we hypothesized that Mena isoform expression would similarly affect the final step in metastatic progression: the formation of spontaneous metastasis. Spontaneous metastases to the lungs were scored in mice with mammary tumors at either 3 or 4 weeks after mammary gland injection of GFP-, Mena11a- and Mena^{INV}-expressing cells. Expression of Mena^{INV} increased the incidence of metastasis compared with expression of GFP and Mena11a, whereas expression of Mena11a decreased metastases after 3 weeks of tumor growth (Fig. 5C). However, after 4 weeks of tumor growth, all primary tumors resulted in detectable metastases regardless of the Mena isoform expressed (Fig. 5C). In addition, Mena^{INV} expression promoted metastatic spread to the lungs with little (at 3 weeks) or no (at 4 weeks) effect on primary tumor growth (supplementary material Fig. S6A,B) (Philippar et al., 2008) or cell growth in vitro (supplementary material Fig. S6C). Hence, differences in tumor metastasis occurring in tumors

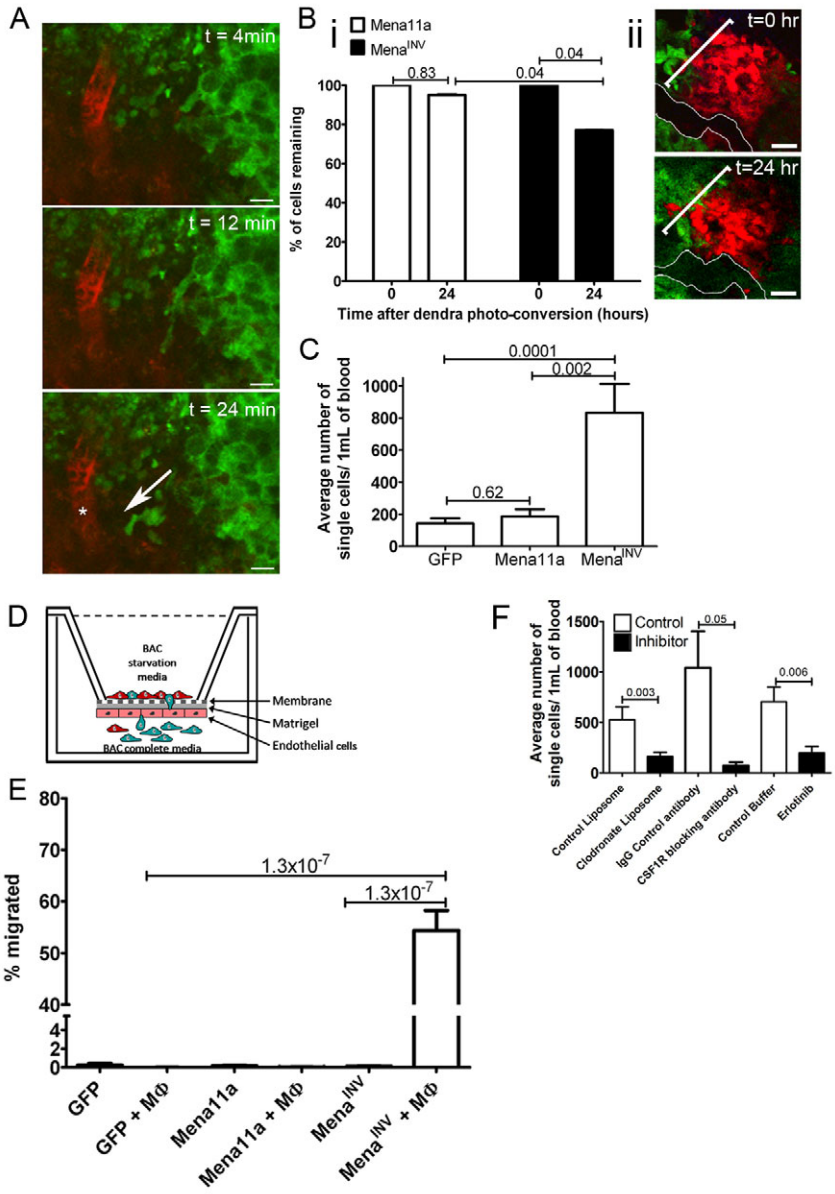

Fig. 4. Mena^{INV} cells promote macrophage-dependent transendothelial migration. (**A**) Multiphoton microscopy of MTLn3–EGFP–Mena^{INV} cells moving towards a blood vessel within the primary mammary tumor of a mouse over 30 minutes. Scale bars: 25 µm. Green, MTLn3–EGFP–Mena^{INV}. Red, Texas Red dextran-labeled blood vessels. White arrow indicates direction of cell movement. Asterisk indicates location of blood vessel. See supplementary material Movie 5. (**Bi**) Quantification of percentage of Denra2 photoconverted tumor cells remaining in the converted area located near a vessel at 0 and 24 hours. (**Bii**) Multiphoton microscopy of a primary tumor. Images taken at 20× over 30 minutes. Red area, Dendra2 photoconverted Mena^{INV} tumor cells at 0 and 24 hours. Green, Dendra2–Mena^{INV} tumor cells. White outline, blood vessel. White bracket indicates area evaluated at each time point. Scale bars: 50 µm. (**C**) Average number of single cells from 1 ml of blood from mice with GFP, Mena^{INV} and Mena11a mammary xenografts; n=10 animals per condition. (**D**) Cartoon depicting TEM assay. Pink cells, endothelial cells. Solid gray line, Matrigel. Dotted gray line, transwell membrane. Red cells, macrophages (BAC1.2 cells). Green cells, carcinoma cells. (**E**) Quantification of TEM of each cell type in the absence or presence of macrophages (MΦ); n=3 experiments each done in duplicate. (**F**) Average number of circulating carcinoma cells in tumors derived from injection of MTLn3–EGFP–Mena^{INV} cells following the indicated treatment; n=10 experiments per condition. P values indicated above bars. Error bars indicate s.e.m.

with different Mena isoform expression are not an indirect consequence of tumor growth. These data indicate that the increased incidence of spontaneous metastasis observed in Mena^{INV}-expressing tumors is due to metastatic events occurring prior to extravasation.

Discussion

Increased Mena expression is correlated with metastasis in breast cancer patients (Di Modugno et al., 2006). In particular, during invasion and migration of tumor cells, expression of Mena^{INV} increases whereas that of Mena11a decreases (Goswami et al., 2009). In this study, we have identified invasion, migration and intravasation as crucial steps of metastasis that are affected by expression of Mena^{INV}- and Mena11a-expressing tumor cells. A key characteristic of Mena^{INV}-expressing cells is their contribution to cell streaming and enhanced intravasation as a result of the dramatic increase in transendothelial migration. Another important finding is the effect of Mena^{INV} expression on tumor cell sensitivity to macrophage-supplied EGF and the subsequent enhancement of paracrine-mediated invasion. Our findings ultimately suggest that the EGF-dependent enhancement of invasion and intravasation in Mena^{INV}-expressing tumor cells contributes to increased tumor cell dissemination and spontaneous metastasis to the lungs.

Conversely, we found that Mena11a-expressing cells do not show dramatically increased streaming and fail to co-invade with macrophages, which indicates a reduced paracrine signaling interaction. The decrease in CSF1 expression in Mena11a-expressing cells contributes to impaired paracrine signaling and leads to the observed deficits that depend on this paracrine signaling loop in vivo, including streaming, invasion, transendothelial migration, tumor cell dissemination and spontaneous metastasis to the lungs.

During invasion, tumor cells are known to decrease their expression of Mena11a and begin producing the Mena^{INV} isoform (Goswami et al., 2009). We have shown that Mena11a expression is correlated with decreased EGF-induced in vivo invasion. We

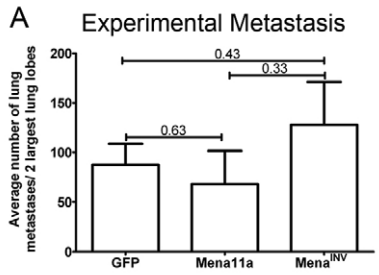

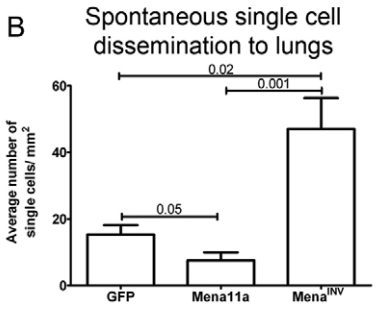

C

Incidence of spontaneous lung metastasis		
	Time for tumor growth:	
Cell type injected:	3 weeks	4 weeks
GFP	3/10 (30%)	10/10 (100%)
Mena11a	1/10 (10%)	10/10 (100%)
Mena^{INV}	6/10 (60%)	10/10 (100%)

Fig. 5. Mena^{INV} enhances dissemination of tumor cells and spontaneous metastasis to the lungs. (**A**) Experimental lung metastasis quantified after intravenous injection of GFP-, Mena11a- or Mena^{INV}-expressing cells showing no statistically significant difference; n=10 animals per cell type. (**B**) Average number of single tumor cells disseminated into the lungs of mice with GFP, Mena11a or Mena^{INV} mammary xenografts; n=10 animals per condition. (**C**) Number of animals with spontaneous lung metastases in mice with GFP, Mena11a and Mena^{INV} mammary xenografts following primary tumor growth. P values indicated above bars. Error bars indicate s.e.m.

have also shown that Mena^{INV}-expressing migratory carcinoma cells are highly sensitive to EGF in their protrusion and chemotaxis activities, leading to significantly enhanced in vivo invasion. These activities can result in Mena^{INV}-expressing cell migration towards, and association with, perivascular macrophages, resulting in enhanced transendothelial migration and intravasation.

In addition to decreased EGF-induced in vivo invasion of Mena11a-expressing cells, we also found that these cells express less *CSF1* mRNA. Data from patients suggests that CSF1 and its receptor play crucial roles during progression of breast cancer (Kacinski et al., 1991; Scholl et al., 1994) and that CSF1 and the CSF1R are coexpressed in >50% of breast tumors (Kacinski, 1997). Elevated circulating CSF1 was also suggested to be an indicator of early metastatic relapse in patients with breast cancer, independent of breast cancer subtype (Scholl et al., 1994; Tamimi et al., 2008; Beck et al., 2009). This suggests that lower levels of CSF1 in Mena11a-expressing cells could lead to decreased metastatic progression. The decreased invasion, intravasation and dissemination of Mena11a-expressing cells are consistent with the decrease in expression of CSF1 and the reduced sensitivity to EGF, which would make these cells less likely to participate in a paracrine signaling loop with macrophages.

A major finding of our study is that the expression of Mena^{INV} enhances a form of coordinated cell migration not previously described, where cell migration is spatially and temporally coordinated between carcinoma cells that are not connected by junctions. We call this newly described form of coordinated cell migration ‘streaming’. Streaming differs from previously described forms of coordinated cell migration, which require the stable retention of cell–cell junctions (Sahai, 2005), because streaming cells need not make contact and the velocities of migration are 10–100 times more rapid. Previous studies have shown that in vivo MTLn3 cells express CSF1 and EGFR, but do not produce CSF1R or EGF, whereas macrophages express CSF1R and EGF but do not produce CSF1 or EGFR (Goswami et al., 2005). Therefore coordinated arms of the paracrine signaling pathways are active in both cell types during invasion in vivo (Wyckoff et al., 2004). In our study, we demonstrate that streaming requires paracrine chemotaxis between carcinoma cells and macrophages. The ability of Mena^{INV}-expressing cells to protrude and chemotax to 25- to 50-fold lower concentrations of EGF than parental tumor cells, and to suppress cell turning in streams, undoubtedly contributes to the extraordinary coordination and maintenance of high velocity migration as cell streams in vivo. We propose that the increased sensitivity of Mena^{INV}-expressing cells to EGF in the EGF–CSF1 paracrine loop is responsible for the increase in streaming motility. This conclusion is supported by the inhibition of streaming following blocking of the EGFR by Erlotinib, or of CSF1R by α-CSF1R (Fig. 3D).

Invasive tumor cells from PyMT mice exhibit increased Mena^{INV} expression and decreased expression of Mena11a (Goswami et al., 2009). Interestingly, recent studies using intravital imaging of mammary tumors in Mena-deficient PyMT mice have shown significantly decreased streaming motility of tumor cells, providing further evidence that Mena contributes to enhanced motility (Roussos et al., 2010). Finally, mammary tumors derived from the human breast cancer cell line, MDA-MB-231, have tumor cells that participate in macrophage–tumor cell paracrine-mediated invasion (Patsialou et al., 2009), and these invasive tumor cells have also been shown to differentially upregulate Mena^{INV} and downregulate Mena11a (Goswami et al., 2009). Together, these findings suggest that paracrine-mediated carcinoma cell streaming is a generalized phenomenon that occurs in rat, mouse and human models of breast cancer and is a consequence of the differential regulation of the Mena isoforms.

In our study, the suppression of invasion and streaming by the inhibition of paracrine signaling between macrophages and tumor cells in vivo, and by decreasing macrophage function in vivo, demonstrates the crucial role of macrophages during coordinated migration of Mena^{INV}-expressing cells (Wyckoff et al., 2007; Hernandez et al., 2009). We also demonstrate that macrophages are essential for transendothelial migration of Mena^{INV}-expressing tumor cells. Our results are consistent with previous work showing that paracrine signaling between tumor cells and macrophages, and the presence of perivascular macrophages in the primary tumor, are required for invasion and intravasation, respectively (Wyckoff et al., 2004; Wyckoff et al., 2007). In particular, our results support previous work suggesting that Mena^{INV}- but not Mena11a-expressing tumor cells specifically contribute to intravasation of breast cancer cells in humans by helping to assemble the macrophage-dependent intravasation compartment called TMEM (Robinson et al., 2009; Roussos et al., 2011).

In vivo, we have shown that Mena^{INV}-expressing cells invade towards very low concentrations of EGF in macrophage-dependent paracrine chemotaxis. In vitro, low concentrations of EGF such as that found in serum, lead to macrophage-independent 3D invasion of Mena^{INV}-expressing cells (Philippar et al., 2008), whereas completion of transendothelial migration requires EGF supplied by macrophages (Wyckoff et al., 2004). The effects of Mena^{INV} expression on EGF-dependent processes lead to increased invasion, intravasation, dissemination and metastasis to the lungs. These data suggest that drugs directed specifically to the inhibition of Mena^{INV}-dependent increased EGF sensitivity will disrupt the paracrine interactions with macrophages required for metastasis, and result in the inhibition of metastasis in mammary tumors.

In this regard, it will be important to understand how the Mena isoforms differ functionally. The INV exon is inserted just after the EVH1 domain, which is primarily responsible for the subcellular localization of Ena/VASP proteins and interactions with several signaling proteins such as Lamellipodin (Gertler et al., 1996; Urbanelli et al., 2006; Pula and Krause, 2008). It is therefore possible that the INV exon might influence the function of Mena^{INV} by regulating its EVH1-mediated interactions (Niebuhr et al., 1997; Boeda et al., 2007). The 11a exon is inserted within the EVH2 domain between the F-actin binding motif and the coiled-coil tetramerization site. F-actin binding is crucial for almost all known Ena/VASP functions, including localization to the tips of lamellipods and the ability to drive filopod and lamellipod formation and extension (Gertler et al., 1996; Loureiro et al., 2002; Applewhite et al., 2007). In vitro, F-actin binding is required for the anti-capping activity of Ena/VASP and is disrupted by phosphorylation at nearby sites (Barzik et al., 2005), as is F-actin bundling. Because 11a is inserted in the analogous region of Mena, it will be interesting to determine whether the barbed end capture activity is affected. Because the 11a insertion is phosphorylated (Di Modugno et al., 2006), it is possible that inclusion of the 11a exon provides a regulatory mechanism for Mena11a.

Future studies will be needed to investigate the molecular and biochemical mechanisms of action of the Mena^{INV} and Mena11a isoforms and their potential utility as a prognostic marker for patient outcome, and as a therapeutic target for breast cancer metastasis.

Materials and Methods

Cell lines

We used MTLn3 cells derived from metastatic lung lesions from rat mammary adenocarcinoma derived following dietary administration of 7,12-dimethylbenz[α]anthracene (tumor line 13762) (Neri et al., 1982). The in vivo biologic characteristics and metastatic potential of these cells have been determined in previous studies and show that MTLn3 cells have a high metastatic potential (Neri et al., 1982; Welch et al., 1983). Western blots, immunofluorescence and fluorescence-activated cell sorting (FACS) confirm that MTLn3 cells express ErbB2, ErbB3 (Levea et al., 2000; Xue et al., 2006; Kedrin et al., 2009) and ErbB4 (personal communication Sumanta Goswami, Yeshiva University, and Michele Balsamo, MIT, Cambridge, MA). Previous studies have also confirmed that EGFRs in MTLn3 cells are fully active and homogenously distributed on the plasma membrane (Lichtner et al., 1992; Bailly et al., 2000). Dominant coexpression of vimentin and CK14 in MTLn3 cells suggests that these cells represent a myoepithelial or basal cell that has partially dedifferentiated (Lichtner et al., 1991). Additionally, MTLn3 cells have been shown to have increased expression of EGFR as compared with the non-metastatic MTC clone derived from the same mouse model (Lichtner et al., 1995; Levea et al., 2000). Taken together, these data indicate that MTLn3 cells have a phenotype similar to basal-like tumors. MTLn3 cells were used in these experiments because they are known to metastasize to the lung when injected into the mammary gland of SCID mice and thus are suitable for metastatic studies. Additionally, these cells have been used to study metastasis by several laboratories, and Mena isoforms in particular (Wyckoff et al., 2000b; Wyckoff et al., 2000a; Sahai, 2005; Philippar et al., 2008; Le Devedec et al., 2010).

Molecular cloning, infection, FACS and cell culture

EGFP–Mena splice isoforms were subcloned into the retroviral vector packaging Murine stem cell virus–EGFP using standard techniques. MTLn3 cells were used for all of the experiments described. MTLn3–Cerulean EGFP–Mena splice isoforms were created using a lentiviral system pCCLsin.PPT.hPGK.Cerulean.pre (courtesy of Sanjeev Gupta, Albert Einstein College of Medicine). MTLn3-Dendra2 cells were created using a Dendra2 cloning vector C1 with G418 selection marker (courtesy of Vladislav Verkhusha, Albert Einstein College of Medicine). Transfection of Dendra2 into MTLn3–EGFP–Mena^{INV} and MTLn3–EGFP–Mena11a cells lines was done using Lipofectamine 2000 (Invitrogen). Retroviral packaging was performed as previously described (Bear et al., 2000). MTLn3–EGFP–Mena^{INV} and MTLn3–EGFP–Mena11a cell lines were FACS sorted to a level of fourfold overexpression of each fusion protein. Sorting of all other cells was done using FACS 72 hours after transfection. The 10% brightest population of infected cell lines were kept for culturing, and selection was maintained using 500 μg/ml G418 geneticin (Invitrogen) when necessary. MTLn3 cells were cultured in α-modified minimum essential medium (α-MEM) supplemented with 5% fetal bovine serum (FBS) and 0.5% PenStrep (Invitrogen).

Animal model and assays for metastatic progression

In vivo studies were performed in orthotopic tumors derived from injection of MTLn3 rat adenocarcinoma cells into SCID mice. MTLn3 cells were engineered to express either EGFP (for controls) or Mena isoform EGFP-fusion proteins: EGFP–Mena^{INV} (Mena^{INV}) and EGFP–Mena11a (Mena11a) at roughly four times the normal level, consistent with the level of spontaneous Mena upregulation in invasive tumor cells in vivo (Philippar et al., 2008; Goswami et al., 2009). SCID mice with tumors derived from injection of these cells into the mammary gland are referred to as GFP, Mena^{INV} or Mena11a xenografts. Tumor cell blood burden was evaluated following 4 weeks of tumor growth as previously described (Wyckoff et al., 2000b). Briefly, blood was drawn from the right ventricle of anesthetized mice and cells were plated in α-MEM media. Following 7 days of cell culture, tumor cells were counted. All cells counted were GFP-positive, confirming their identity as tumor cells. To functionally impair macrophages, mice were treated with 100 μl of PBS (control) or clodronate (Cl2MDP)-containing liposomes per 10 g of weight via tail vein injection 24 hours prior to collection of blood (Hernandez et al., 2009). Liposomes were prepared as previously described using a clodronate concentration of 2.5 g/10 ml of PBS (van Rooijen and van Kesteren-Hendrikx, 2003). Clodronate was a gift of Roche Diagnostics (Mannheim, Germany). Phosphatidylcholine (Lipoid E PC) was obtained from Lipoid (Ludwigshafen, Germany). Cholesterol was purchased from Sigma. Mice were treated with CSF1R blocking antibody or IgG antibody 4 hours prior to collection of blood to block signaling between tumor cells and macrophages (Wyckoff et al., 2004). Single tumor cell dissemination to the lung was quantified ex vivo using epifluorescence in ten random high power fields per set of mouse lungs at 3 weeks after mammary gland injection of each cell line. Spontaneous lung metastases (>2 mm) were evaluated ex vivo using epifluorescence at 3 and 4 weeks after mammary gland injection of Mena^{INV}- or Mena11a-expressing cells as previously described (Philippar et al., 2008). Experimental metastases were evaluated ex vivo 2 weeks after tail vein injection of 5×10^5 cells of each cell type as previously described (Wang et al., 2006). Lungs were examined using a 60× 1.2 NA water immersion correction lens on an inverted Olympus IX70 (Wyckoff et al., 2000b). For each experiment described above, 10–15 animals were used per Mena isoform cell type. All experiments involving animals were approved by the Einstein Institute for Animal Studies.

In vivo invasion assay and in vitro 3D invasion assay

The in vivo invasion assay was performed in 5–10 mice per condition as previously described (Wyckoff et al., 2000a). We have previously measured the ranges of EGF and CSF1 concentrations required to initiate chemotaxis and migration in vivo (Wyckoff et al., 2004; Patsialou et al., 2009; Raja et al., 2010). The concentrations shown to be effective and used in our study vary from 50% to 10% of the K_d of these ligands for their respective receptors. In addition, these are the concentrations believed to be present in vivo (Byyny et al., 1974; Bartocci et al., 1986). The paracrine loop was inhibited using 10 μg of affinity-purified α-mouse CSF1R-blocking antibody (α-CSF1R; courtesy of Richard Stanley, Yeshiva University, Bronx, NY) or 6.25 nM Erlotinib (gift from OSI Pharmaceuticals, Melvile, NY), empirically determined by OSI Pharmaceuticals, dissolved in DMSO in needles containing 25 nM and 1 nM EGF for GFP- and Mena^{INV}-expressing cells, respectively (Wyckoff et al., 2004); α-rat IgG or DMSO were used as controls, respectively. Cells were imaged on an Olympus IX70 inverted microscope with a 10× NA 0.30 objective. For in vivo invasion experiments performed with EGFR (Erlotinib) and CSF1R inhibitors, we used 1 nM EGF in the needles inserted into Mena^{INV}-expressing tumors and 25 nM EGF in the needles inserted into GFP-expressing tumors to allow maximal tumor cell collection (350–600 cells collected per needle) (Philippar et al., 2008). In vitro 3D invasion assays were performed as previously described (Goswami et al., 2005).

Intravital imaging

Intravital multiphoton imaging was performed as described previously (Wang et al., 2002; Wyckoff et al., 2010) using a 20× 1.95 NA water immersion objective with

correction lens. Time-lapse movies were analyzed for frequency of motility and tracking, and for measuring and quantifying of cell characteristics in 3D and through time using NIH ImageJ (Sahai et al., 2005) and custom software described elsewhere (Wyckoff et al., 2010). A cell movement event was defined as a translocation of >1 cell diameter (25 μm) observed within a visual field that is defined in three dimensions as 100 μm by 512×512 pixels per minute. Streaming cells were quantified as the number of individual carcinoma cells in a field whose vector paths point in the same direction (Fig. 1A). Random cells movements were quantified as the number of individual carcinoma cells in a field whose vector paths point in different directions (Fig. 1A). To confirm the elimination of macrophages in clodronate-treated mice, multiphoton microscopy of spleens removed from both clodronate- and PBS liposome-treated animals was performed as previously described (Hernandez et al., 2009). Mice were given intraperitoneal injection of 10 mg/kg body weight of vehicle (6% Captisol) or Erlotinib in 6% Captisol, 2 hours prior to IVI, or 2.5 μg of CSF1R-blocking anitbody or IgG in PBS 4 hours prior to IVI. Tail vein injection of 200 μl 70 kDa Texas Red dextran was used to label blood vessels, which were immediately visualized following injection. After 2 hours, macrophages were also labeled with dextran as previously described (Wyckoff et al., 2007).

Mammary imaging windows were placed over the mammary gland of mice 3 weeks after injection of carcinoma cells (Kedrin et al., 2008). Photoconversion of the Dendra2 variant from green to red was done using a 405 nm UV laser on a Leica TCS SP2 AOBS confocal microscope (Mannheim, Germany) equipped with a 20× glycerol objective (Kedrin et al., 2008). Z-stacks (~100 μm deep) of the same fields were imaged at 0 and 24 hours after photoconversion in imaging sessions using a multiphoton microscope equipped with a MaiTai 15 W laser tuned to 1045 nm for red Dendra2 and a Tsunami 15 W laser tuned to 880 nm for green Dendra2 (Kedrin et al., 2008). Quantification of intravasation was done as previously described (Kedrin et al., 2008).

Real time PCR

RNA was extracted from all cell lines at steady state, and quantitative real time PCR was performed as previously described (Goswami et al., 2009). Primers designed against Rat EGFR and CSF1 were used to determine levels of expression of each. Primer sequences used for EGFR: rEGFR forward 5′-TCGTTGCCGACGCAGT-CACC-3′, rEGFR reverse 5′-TCCCTGAGGGTCGCATCCCG-3′. Primer sequences used for CSF1: rCSF-1 forward 5′-GCTCGAGGGCAAGAAAAGTA-3′, rCSF-1 reverse 5′-CCTGTGTCGGTCAAAGGAAT-3′.

Transendothelial migration assay

To prepare the endothelial monolayer, the underside of each transwell was coated with 50 μl of 2.5 μg/ml Matrigel (Invitrogen). Some 200,000 rat pulmonary microvascular endothelial cells (RLE) were plated in 50 μl of DMEM + 10% FBS (medium 1) and incubated at 37°C for 4 hours. Transwells were flipped onto a 24-well plate containing 1 or 200 μl of medium 1 in the lower or upper chambers, respectively. BAC1.2F5 macrophages and tumor cells were labeled with cell-tracker dyes. Then, 15,000 macrophages and 37,500 tumor cells were added to the upper chamber in 200 μl of α-MEM + 0.5% FBS (medium 2), and 200 μl of α-MEM + 10% FBS + 3000 units CSF1 were added to the lower chamber. Following 18 hours of transmigration, medium was removed from the top of the transwell and migrated cells were scraped from the bottom of the plate. Cells were fixed in 0.1% formaldehyde and analyzed using a Guava flow cytometer. Monolayers were tested for permeability both before and after cell migration via quantification of fluorescence (Molecular Devices SpectraMax M5 plate reader) of 70 kDa rhodamine-dextran in the media from both upper and lower transwell chambers added 24 hours prior.

Immunohistochemistry

Primary tumors were fixed in 10% buffered formalin, and paraffin embedded. Sections of 10 μm were cut and placed on slides for further staining. Immunohistochemistry was carried out using α-GFP at 1:200 to identify tumor cells containing GFP-fusion proteins, and rat α-F4/80 (courtesy of Jeffrey Pollard, Albert Einstein College of Medicine) was used at 1:25 to identify macrophages. All staining was done using standard protocols, and eosin was used as a nuclear counterstain. Slides were analyzed and imaged using Zeiss AxioObserver.Z1 5× DIC1, EC Plan-Neofluar 10×/0.3 Ph1, EC Plan-Neofluar 20×/0.5 Ph2 M27, EC Plan-Neofluar 40×/0.75 Ph2 M27, EC Plan-neofluar 63×/1.4 Oil and an AxioCamHR3.

Statistical analysis

For all experiments, statistical significances were determined using unpaired, two-tailed Student's *t*-tests assuming equal variances and an alpha level of 0.05 unless otherwise specified. Differences were considered significant for $P<0.05$. For assessment of lung metastasis and circulating tumor cells, the non-parametric Mann Whitney Wilcoxon rank sum test was used.

We would like to thank Diane Cox, Antonia Patsialou, and Daqian Sun for stimulating discussion and helpful suggestions. We would also like to thank Richard Stanley (Albert Einstein College of Medicine, Yeshiva University, Bronx, NY) for his generous contribution of CSF1R blocking antibody as well as OSI Pharmaceuticals (Melville, NY) for their generous donation of Erlotinib. Many thanks to David Entenberg and Jenny Tadros for their technical support, Einstein histopathology and analytical imaging facilities and Koch Institute Microscopy core facility for their services. Grant support was provided by NIH-CA100324 (A.R.B., J.B.W., Y.W. S.G., J.E.S.), NIH-CA126511 (B.G.), NIH-CA150344 (E.T.R., J.S.C.), NIH-CA77522 (J.E.S.), Ludwig Fund postdoctoral fellowship (M.B.), DoD CDMRP BCRP Fellowship (BC087781) (S.K.A.), NIH-GM58801 and funds from the Ludwig Center at MIT (F.B.G.), ICBP grant U54 CA112967 (D.A.L., F.B.G.) and the Charles H. Revson Fellowship (B.G.). None of the authors have any conflicts of interest. Data in this paper are from a thesis to be submitted in partial fulfillment of the requirements for the Degree of Doctor of Philosophy in the Graduate Division of Medical Sciences, Albert Einstein College of Medicine, Yeshiva University. Deposited in PMC for release after 12 months.

Supplementary material available online at
http://jcs.biologists.org/cgi/content/full/124/13/2120/DC1

References

Andresen, V., Alexander, S., Heupel, W. M., Hirschberg, M., Hoffman, R. M. and Friedl, P. (2009). Infrared multiphoton microscopy: subcellular-resolved deep tissue imaging. *Curr. Opin. Biotechnol.* **20**, 54-62.

Applewhite, D. A., Barzik, M., Kojima, S., Svitkina, T. M., Gertler, F. B. and Borisy, G. G. (2007). Ena/VASP proteins have an anti-capping independent function in filopodia formation. *Mol. Biol. Cell* **18**, 2579-2591.

Bailly, M., Wyckoff, J., Bouzahzah, B., Hammerman, R., Sylvestre, V., Cammer, M., Pestell, R. and Segall, J. E. (2000). Epidermal growth factor receptor distribution during chemotactic responses. *Mol. Biol. Cell* **11**, 3873-3883.

Bartocci, A., Pollard, J. W. and Stanley, E. R. (1986). Regulation of colony-stimulating factor 1 during pregnancy. *J. Exp. Med.* **164**, 956-961.

Barzik, M., Kotova, T. I., Higgs, H. N., Hazelwood, L., Hanein, D., Gertler, F. B. and Schafer, D. A. (2005). Ena/VASP proteins enhance actin polymerization in the presence of barbed end capping proteins. *J. Biol. Chem.* **280**, 28653-28662.

Bear, J. E. and Gertler, F. B. (2009). Ena/VASP: towards resolving a pointed controversy at the barbed end. *J. Cell Sci.* **122**, 1947-1953.

Bear, J. E., Loureiro, J. J., Libova, I., Fassler, R., Wehland, J. and Gertler, F. B. (2000). Negative regulation of fibroblast motility by Ena/VASP proteins. *Cell* **101**, 717-728.

Bear, J. E., Svitkina, T. M., Krause, M., Schafer, D. A., Loureiro, J. J., Strasser, G. A., Maly, I. V., Chaga, O. Y., Cooper, J. A., Borisy, G. G. et al. (2002). Antagonism between Ena/VASP proteins and actin filament capping regulates fibroblast motility. *Cell* **109**, 509-521.

Beck, A. H., Espinosa, I., Edris, B., Li, R., Montgomery, K., Zhu, S., Varma, S., Marinelli, R. J., van de Rijn, M. and West, R. B. (2009). The macrophage colony-stimulating factor 1 response signature in breast carcinoma. *Clin. Cancer Res.* **15**, 778-787.

Boeda, B., Briggs, D. C., Higgins, T., Garvalov, B. K., Fadden, A. J., McDonald, N. Q. and Way, M. (2007). Tes, a specific Mena interacting partner, breaks the rules for EVH1 binding. *Mol. Cell* **28**, 1071-1082.

Byyny, R. L., Orth, D. N., Cohen, S. and Doyne, E. S. (1974). Epidermal growth factor: effects of androgens and adrenergic agents. *Endocrinology* **95**, 776-782.

Condeelis, J. and Pollard, J. W. (2006). Macrophages: obligate partners for tumor cell migration, invasion, and metastasis. *Cell* **124**, 263-266.

Condeelis, J. and Segall, J. E. (2003). Intravital imaging of cell movement in tumours. *Nat. Rev. Cancer* **3**, 921-930.

Di Modugno, F., Mottolese, M., Di Benedetto, A., Conidi, A., Novelli, F., Perracchio, L., Venturo, I., Botti, C., Jager, E., Santoni, A. et al. (2006). The cytoskeleton regulatory protein hMena (ENAH) is overexpressed in human benign breast lesions with high risk of transformation and human epidermal growth factor receptor-2-positive/hormonal receptor-negative tumors. *Clin. Cancer Res.* **12**, 1470-1478.

Di Modugno, F., DeMonte, L., Balsamo, M., Bronzi, G., Nicotra, M. R., Alessio, M., Jager, E., Condeelis, J. S., Santoni, A., Natali, P. G. et al. (2007). Molecular cloning of hMena (ENAH) and its splice variant hMena+11a: epidermal growth factor increases their expression and stimulates hMena+11a phosphorylation in breast cancer cell lines. *Cancer Res.* **67**, 2657-2665.

Egeblad, M., Ewald, A. J., Askautrud, H. A., Truitt, M. L., Welm, B. E., Bainbridge, E., Peeters, G., Krummel, M. F. and Werb, Z. (2008). Visualizing stromal cell dynamics in different tumor microenvironments by spinning disk confocal microscopy. *Dis. Model. Mech.* **1**, 155-167; discussion 165.

Ferron, F., Rebowski, G., Lee, S. H. and Dominguez, R. (2007). Structural basis for the recruitment of profilin-actin complexes during filament elongation by Ena/VASP. *EMBO J.* **26**, 4597-4606.

Friedl, P. and Wolf, K. (2010). Plasticity of cell migration: a multiscale tuning model. *J. Cell Biol.* **188**, 11-19.

Gaggioli, C., Hooper, S., Hidalgo-Carcedo, C., Grosse, R., Marshall, J. F., Harrington, K. and Sahai, E. (2007). Fibroblast-led collective invasion of carcinoma cells with differing roles for RhoGTPases in leading and following cells. *Nat. Cell Biol.* **9**, 1392-1400.

Gertler, F. B., Niebuhr, K., Reinhard, M., Wehland, J. and Soriano, P. (1996). Mena, a relative of VASP and Drosophila Enabled, is implicated in the control of microfilament dynamics. *Cell* **87**, 227-239.

Giampieri, S., Manning, C., Hooper, S., Jones, L., Hill, C. S. and Sahai, E. (2009). Localized and reversible TGFbeta signalling switches breast cancer cells from cohesive to single cell motility. *Nat. Cell Biol.* **11**, 1287-1296.

Goswami, S., Wang, W., Wyckoff, J. B. and Condeelis, J. S. (2004). Breast cancer cells isolated by chemotaxis from primary tumors show increased survival and resistance to chemotherapy. *Cancer Res.* **64**, 7664-7667.

Goswami, S., Sahai, E., Wyckoff, J. B., Cammer, M., Cox, D., Pixley, F. J., Stanley, E. R., Segall, J. E. and Condeelis, J. S. (2005). Macrophages promote the invasion of breast carcinoma cells via a colony-stimulating factor-1/epidermal growth factor paracrine loop. *Cancer Res.* **65**, 5278-5283.

Goswami, S., Philippar, U., Sun, D., Patsialou, A., Avraham, J., Wang, W., Di Modugno, F., Nistico, P., Gertler, F. B. and Condeelis, J. S. (2009). Identification of invasion specific splice variants of the cytoskeletal protein Mena present in mammary tumor cells during invasion in vivo. *Clin. Exp. Metastasis* **26**, 153-159.

Gurzu, S., Jung, I., Prantner, I., Ember, I., Pavai, Z. and Mezei, T. (2008). The expression of cytoskeleton regulatory protein Mena in colorectal lesions. *Rom. J. Morphol. Embryol.* **49**, 345-349.

Gurzu, S., Jung, I., Prantner, I., Chira, L. and Ember, I. (2009). The immunohistochemical aspects of protein Mena in cervical lesions. *Rom. J. Morphol. Embryol.* **50**, 213-216.

Hansen, S. D. and Mullins, R. D. (2010). VASP is a processive actin polymerase that requires monomeric actin for barbed end association. *J. Cell Biol.* **191**, 571-584.

Hernandez, L., Smirnova, T., Kedrin, D., Wyckoff, J., Zhu, L., Stanley, E. R., Cox, D., Muller, W. J., Pollard, J. W., Van Rooijen, N. et al. (2009). The EGF/CSF-1 paracrine invasion loop can be triggered by heregulin beta1 and CXCL12. *Cancer Res.* **69**, 3221-3227.

Ilina, O. and Friedl, P. (2009). Mechanisms of collective cell migration at a glance. *J. Cell Sci.* **122**, 3203-3208.

Kacinski, B. M. (1997). CSF-1 and its receptor in breast carcinomas and neoplasms of the female reproductive tract. *Mol. Reprod. Dev.* **46**, 71-74.

Kacinski, B. M., Scata, K. A., Carter, D., Yee, L. D., Sapi, E., King, B. L., Chambers, S. K., Jones, M. A., Pirro, M. H., Stanley, E. R. et al. (1991). FMS (CSF-1 receptor) and CSF-1 transcripts and protein are expressed by human breast carcinomas in vivo and in vitro. *Oncogene* **6**, 941-952.

Kedrin, D., van Rheenen, J., Hernandez, L., Condeelis, J. and Segall, J. E. (2007). Cell motility and cytoskeletal regulation in invasion and metastasis. *J. Mammary Gland Biol. Neoplasia* **12**, 143-152.

Kedrin, D., Gligorijevic, B., Wyckoff, J., Verkhusha, V. V., Condeelis, J., Segall, J. E. and van Rheenen, J. (2008). Intravital imaging of metastatic behavior through a mammary imaging window. *Nat. Methods* **5**, 1019-1021.

Kedrin, D., Wyckoff, J., Boimel, P. J., Coniglio, S. J., Hynes, N. E., Arteaga, C. L. and Segall, J. E. (2009). ERBB1 and ERBB2 have distinct functions in tumor cell invasion and intravasation. *Clin. Cancer Res.* **15**, 3733-3739.

Le Devedec, S. E., van Roosmalen, W., Maria, N., Grimbergen, M., Pont, C., Lalai, R. and van de Water, B. (2009). An improved model to study tumor cell autonomous metastasis programs using MTLn3 cells and the Rag2(–/–) gammac (–/–) mouse. *Clin. Exp. Metastasis* **26**, 673-684.

Le Devedec, S. E., Lalai, R., Pont, C., de Bont, H. and van de Water, B. (2010). Two-photon intravital multicolor imaging combined with inducible gene expression to distinguish metastatic behavior of breast cancer cells in vivo. *Mol. Imaging Biol.* **13**, 67-77.

Levea, C. M., McGary, C. T., Symons, J. R. and Mooney, R. A. (2000). PTP LAR expression compared to prognostic indices in metastatic and non-metastatic breast cancer. *Breast Cancer Res. Treat.* **64**, 221-228.

Lichtner, R. B., Julian, J. A., Glasser, S. R. and Nicolson, G. L. (1989). Characterization of cytokeratins expressed in metastatic rat mammary adenocarcinoma cells. *Cancer Res.* **49**, 104-111.

Lichtner, R. B., Julian, J. A., North, S. M., Glasser, S. R. and Nicolson, G. L. (1991). Coexpression of cytokeratins characteristic for myoepithelial and luminal cell lineages in rat 13762NF mammary adenocarcinoma tumors and their spontaneous metastases. *Cancer Res.* **51**, 5943-5950.

Lichtner, R. B., Wiedemuth, M., Kittmann, A., Ullrich, A., Schirrmacher, V. and Khazaie, K. (1992). Ligand-induced activation of epidermal growth factor receptor in intact rat mammary adenocarcinoma cells without detectable receptor phosphorylation. *J. Biol. Chem.* **267**, 11872-11880.

Lichtner, R. B., Kaufmann, A. M., Kittmann, A., Rohde-Schulz, B., Walter, J., Williams, L., Ullrich, A., Schirrmacher, V. and Khazaie, K. (1995). Ligand mediated activation of ectopic EGF receptor promotes matrix protein adhesion and lung colonization of rat mammary adenocarcinoma cells. *Oncogene* **10**, 1823-1832.

Loureiro, J. J., Rubinson, D. A., Bear, J. E., Baltus, G. A., Kwiatkowski, A. V. and Gertler, F. B. (2002). Critical roles of phosphorylation and actin binding motifs, but not the central proline-rich region, for Ena/vasodilator-stimulated phosphoprotein (VASP) function during cell migration. *Mol. Biol. Cell* **13**, 2533-2546.

Neri, A., Welch, D., Kawaguchi, T. and Nicolson, G. L. (1982). Development and biologic properties of malignant cell sublines and clones of a spontaneously metastasizing rat mammary adenocarcinoma. *J. Natl. Cancer Inst.* **68**, 507-517.

Niebuhr, K., Ebel, F., Frank, R., Reinhard, M., Domann, E., Carl, U. D., Walter, U., Gertler, F. B., Wehland, J. and Chakraborty, T. (1997). A novel proline-rich motif present in ActA of Listeria monocytogenes and cytoskeletal proteins is the ligand for the EVH1 domain, a protein module present in the Ena/VASP family. *EMBO J.* **16**, 5433-5444.

Pasic, L., Kotova, T. and Schafer, D. A. (2008). Ena/VASP proteins capture actin filament barbed ends. *J. Biol. Chem.* **283**, 9814-9819.

Patsialou, A., Wyckoff, J., Wang, Y., Goswami, S., Stanley, E. R. and Condeelis, J. S. (2009). Invasion of human breast cancer cells in vivo requires both paracrine and autocrine loops involving the Colony-Stimulating Factor-1 receptor. *Cancer Res.* **69**, 9498-9506.

Perentes, J. Y., McKee, T. D., Ley, C. D., Mathiew, H., Dawson, M., Padera, T. P., Munn, L. L., Jain, R. K. and Boucher, Y. (2009). In vivo imaging of extracellular matrix remodeling by tumor-associated fibroblasts. *Nat. Methods* **6**, 143-145.

Philippar, U., Roussos, E. T., Oser, M., Yamaguchi, H., Kim, H. D., Giampieri, S., Wang, Y., Goswami, S., Wyckoff, J. B., Lauffenburger, D. A. et al. (2008). A Mena invasion isoform potentiates EGF-induced carcinoma cell invasion and metastasis. *Dev. Cell* **15**, 813-828.

Pino, M. S., Balsamo, M., Di Modugno, F., Mottolese, M., Alessio, M., Melucci, E., Milella, M., McConkey, D. J., Philippar, U., Gertler, F. B. et al. (2008). Human Mena+11a isoform serves as a marker of epithelial phenotype and sensitivity to epidermal growth factor receptor inhibition in human pancreatic cancer cell lines. *Clin. Cancer Res.* **14**, 4943-4950.

Pula, G. and Krause, M. (2008). Role of Ena/VASP proteins in homeostasis and disease. *Handb. Exp. Pharmacol.* **186**, 39-65.

Raja, W. K., Gligorijevic, B., Wyckoff, J., Condeelis, J. S. and Castracane, J. (2010). A new chemotaxis device for cell migration studies. *Integr. Biol. (Camb.)* **2**, 696-706.

Robinson, B. D., Sica, G. L., Liu, Y. F., Rohan, T. E., Gertler, F. B., Condeelis, J. S. and Jones, J. G. (2009). Tumor microenvironment of metastasis in human breast carcinoma: a potential prognostic marker linked to hematogenous dissemination. *Clin. Cancer Res.* **15**, 2433-2441.

Roussos, E. T., Goswami, S., Balsamo, M., Wang, Y., Stobezki, R., Adler, E., Robinson, B. D., Jones, J. G., Gertler, F. B., Condeelis J. S. et al. (2011). Mena invasive ($Mena^{INV}$) and Mena11a isoforms play distinct roles in breast cancer cell cohesion and association with TMEM. *Clin. Exp. Metastasis* [Epub ahead of print] doi: 10.1007/s10585-011-9388-6.

Roussos, E. T., Wang, Y., Wyckoff, J. B., Sellers, R. S., Wang, W., Li, J., Pollard, J. W., Gertler, F. B. and Condeelis, J. S. (2010). Mena deficiency delays tumor progression and decreases metastasis in polyoma middle-T transgenic mouse mammary tumors. *Breast Cancer Res.* **12**, R101.

Sahai, E. (2005). Mechanisms of cancer cell invasion. *Curr. Opin. Genet. Dev.* **15**, 87-96.

Sahai, E., Wyckoff, J., Philippar, U., Segall, J. E., Gertler, F. and Condeelis, J. (2005). Simultaneous imaging of GFP, CFP and collagen in tumors in vivo using multiphoton microscopy. *BMC Biotechnol.* **5**, 14.

Scholl, S. M., Pallud, C., Beuvon, F., Hacene, K., Stanley, E. R., Rohrschneider, L., Tang, R., Pouillart, P. and Lidereau, R. (1994). Anti-colony-stimulating factor-1 antibody staining in primary breast adenocarcinomas correlates with marked inflammatory cell infiltrates and prognosis. *J. Natl. Cancer Inst.* **86**, 120-126.

Segall, J. E., Tyerech, S., Boselli, L., Masseling, S., Helft, J., Chan, A., Jones, J. and Condeelis, J. (1996). EGF stimulates lamellipod extension in metastatic mammary adenocarcinoma cells by an actin-dependent mechanism. *Clin. Exp. Metastasis* **14**, 61-72.

Tamimi, R. M., Brugge, J. S., Freedman, M. L., Miron, A., Iglehart, J. D., Colditz, G. A. and Hankinson, S. E. (2008). Circulating colony stimulating factor-1 and breast cancer risk. *Cancer Res.* **68**, 18-21.

Urbanelli, L., Massini, C., Emiliani, C., Orlacchio, A. and Bernardi, G. (2006). Characterization of human Enah gene. *Biochim. Biophys. Acta* **1759**, 99-107.

van Rooijen, N. and van Kesteren-Hendrikx, E. (2003). "In vivo" depletion of macrophages by liposome-mediated "suicide". *Methods Enzymol.* **373**, 3-16.

Wang, W., Wyckoff, J. B., Frohlich, V. C., Oleynikov, Y., Huttelmaier, S., Zavadil, J., Cermak, L., Bottinger, E. P., Singer, R. H., White, J. G. et al. (2002). Single cell behavior in metastatic primary mammary tumors correlated with gene expression patterns revealed by molecular profiling. *Cancer Res.* **62**, 6278-6288.

Wang, W., Goswami, S., Lapidus, K., Wells, A. L., Wyckoff, J. B., Sahai, E., Singer, R. H., Segall, J. E. and Condeelis, J. S. (2004). Identification and testing of a gene expression signature of invasive carcinoma cells within primary mammary tumors. *Cancer Res.* **64**, 8585-8594.

Wang, W., Mouneimne, G., Sidani, M., Wyckoff, J., Chen, X., Makris, A., Goswami, S., Bresnick, A. R. and Condeelis, J. S. (2006). The activity status of cofilin is directly related to invasion, intravasation, and metastasis of mammary tumors. *J. Cell Biol.* **173**, 395-404.

Wang, W., Wyckoff, J. B., Goswami, S., Wang, Y., Sidani, M., Segall, J. E. and Condeelis, J. S. (2007). Coordinated regulation of pathways for enhanced cell motility and chemotaxis is conserved in rat and mouse mammary tumors. *Cancer Res.* **67**, 3505-3511.

Welch, D. R., Neri, A. and Nicolson, G. L. (1983). Comparison of 'spontaneous' and 'experimental' metastasis using rat 13762 mammary adenocarcinoma metastatic cell clones. *Invasion Metastasis* **3**, 65-80.

Wolf, K., Mazo, I., Leung, H., Engelke, K., von Andrian, U. H., Deryugina, E. I., Strongin, A. Y., Brocker, E. B. and Friedl, P. (2003). Compensation mechanism in tumor cell migration: mesenchymal-amoeboid transition after blocking of pericellular proteolysis. *J. Cell Biol.* **160**, 267-277.

Wyckoff, J., Wang, W., Lin, E. Y., Wang, Y., Pixley, F., Stanley, E. R., Graf, T., Pollard, J. W., Segall, J. and Condeelis, J. (2004). A paracrine loop between tumor cells and macrophages is required for tumor cell migration in mammary tumors. *Cancer Res.* **64**, 7022-7029.

Wyckoff, J., Gligoijevic, B., Entenberg, D., Segall, J. and Condeelis J. (2010). High-resolution multiphoton imaging of tumors in vivo. In *Live Cell Imaging: A Laboratory*

Manual, 2nd edn (ed. R. D. Goldman, J. R. Swedlow and D. L. Spector), pp. 441-462. Cold Spring Harbor: Cold Spring Harbor Laboratory Press.

Wyckoff, J. B., Segall, J. E. and Condeelis, J. S. (2000a). The collection of the motile population of cells from a living tumor. *Cancer Res.* **60**, 5401-5404.

Wyckoff, J. B., Jones, J. G., Condeelis, J. S. and Segall, J. E. (2000b). A critical step in metastasis: in vivo analysis of intravasation at the primary tumor. *Cancer Res.* **60**, 2504-2511.

Wyckoff, J. B., Wang, Y., Lin, E. Y., Li, J. F., Goswami, S., Stanley, E. R., Segall, J. E., Pollard, J. W. and Condeelis, J. (2007). Direct visualization of macrophage-assisted tumor cell intravasation in mammary tumors. *Cancer Res.* **67**, 2649-2656.

Xue, C., Wyckoff, J., Liang, F., Sidani, M., Violini, S., Tsai, K. L., Zhang, Z. Y., Sahai, E., Condeelis, J. and Segall, J. E. (2006). Epidermal growth factor receptor overexpression results in increased tumor cell motility in vivo coordinately with enhanced intravasation and metastasis. *Cancer Res.* **66**, 192-197.

Yamaguchi, H., Pixley, F. and Condeelis, J. (2006). Invadopodia and podosomes in tumor invasion. *Eur. J. Cell Biol.* **85**, 213-218.

Zerbe, L. K., Dwyer-Nield, L. D., Fritz, J. M., Redente, E. F., Shroyer, R. J., Conklin, E., Kane, S., Tucker, C., Eckhardt, S. G., Gustafson, D. L. et al. (2008). Inhibition by erlotinib of primary lung adenocarcinoma at an early stage in male mice. *Cancer Chemother. Pharmacol.* **62**, 605-620.

Journal of Cell Science